Multiscaling in Randomly Forced Hydrodynamical Equations

Rahul Pandit

Department of Physics, Indian Institute of Science, Bangalore

December 18, 2020

Turbulence: Problems at the Interface of Mathematics and Physics (Online)

International Centre for Theoretical Sciences (ICTS), Bangalore

Acknowledgements

- Support: CSIR, DST, IFCAM, and SERC (IISc).
- C. Jayaprakash, F. Hayot, Anirban Sain, Manu, Dhrubaditya Mitra, Jeremie Bec, Uriel Frisch.
- Ganapati Sahoo, Nadia Bihari Padhan, Abhik Basu, Sadhitro De, Dipankar Roy, Dhrubaditya Mitra, Uriel Frisch

Historical perspectives/Motivation

- Direct numerical simulations indicate that turbulence with (spatial) power-law forcing has at least two different regimes (dependent on the power-law forcing): (a) with scale invariant statistics and (b) with multifractal statistics, i.e., broken scale invariance.
- Can these be studied by using a variant of theories of spontaneous stochasticity, rough paths, and regularity structures, as recently applied to the Kardar Parisi Zhang (KPZ) equation?
- There is a long tradition, in fluid mechanics, of including a driving force in the equations; here we investigate random driving forces.

Historical perspectives/Motivation

- For fundamental investigations, it is convenient to follow Edwards's proposal, which assumes prescribed random driving forces that do not trivially break the scaling invariance of the Euler equation

The statistical dynamics of homogeneous turbulence

By S. F. EDWARDS

Department of Theoretical Physics, University of Manchester, and Culham Laboratories, Culham, Abingdon, Berks.

(Received 2 May 1963)

Historical perspectives/Motivation

- At the time of Edwards's proposal, the renormalization group (RG) was not available.
- The first RG study of fluid turbulence, with such forcing, was performed by Forster, Nelson, and Stephen in 1977; their study did not go far from the threshold for the breaking of scale invariance

PHYSICAL REVIEW A VOLUME 16, NUMBER 2 AUGUST 1977

Large-distance and long-time properties of a randomly stirred fluid

Dieter Forster*
Department of Physics, Temple University, Philadelphia, Pennsylvania 19122

David R. Nelson†
Department of Physics, Harvard University, Cambridge, Massachusetts 02138

Michael J. Stephen‡
Physics Department, Rutgers University, New Brunswick, New Jersey 08903
(Received 14 February 1977)

Historical perspectives/Motivation

- In 1979, de Dominicis and Martin realized that, far from this threshold, K41 scaling might be achieved.
- Many other RG and related studies clarified these ideas.

PHYSICAL REVIEW A VOLUME 19, NUMBER 1 JANUARY 1979

Energy spectra of certain randomly-stirred fluids

C. DeDominicis* and P. C. Martin
Lyman Laboratory of Physics, Harvard University, Cambridge, Massachusetts 02138
(Received 19 June 1978)

Historical perspectives/Motivation

- Some other research in this direction:
  - J.-D. Fournier and U. Frisch, Phys. Rev. A 28, 1000 (1983).
  - V. Yakhot and S. A. Orszag, J. Sci. Comput. 1, 3 (1986).
  - J. K. Bhattacharjee, J. Phys. A 21, L551 (1988).
  - C.-Y. Mou and P.B. Weichman, Phys. Rev. E 52, 3738 (1995).
  - Field Theoretic Renormalization Group in Fully Developed Turbulence, by L.Ts Adzhemyan, N.V. Antonov, A.N. Vasiliev, Gordon and Breach Science Publishers, 1999.

Historical perspectives/Motivation

- In 1998, the explicit breaking of such scale invariance was shown via numerical investigations.

VOLUME 81, NUMBER 20 PHYSICAL REVIEW LETTERS 16 NOVEMBER 1998

Turbulence and Multiscaling in the Randomly Forced Navier-Stokes Equation

Anirban Sain,[1] Manu,[2,*] and Rahul Pandit[1,†]
[1]*Department of Physics, Indian Institute of Science, Bangalore 560 012, India*
[2]*School of Physical Sciences, Jawaharlal Nehru University, New Delhi 110 067, India*
(Received 29 December 1997)

Historical perspectives/Motivation

- The 3D randomly-forced Navier-Stokes equation (3D RFNSE) is as follows:

$$\frac{\partial \mathbf{u}}{\partial t} + (\mathbf{u}\cdot\nabla)\mathbf{u} = -\nabla P + \nu\nabla^2\mathbf{u} + \mathbf{f}\,; \quad \nabla\cdot\mathbf{u} = \mathbf{0}$$

  where $\mathbf{u}(\mathbf{r},\, t)$ is the fluid velocity, P is the pressure, ν is the kinematic viscosity.

- The random force $\mathbf{f}$ is Gaussian, white-in-time and has the following Fourier space correlation:

$$\langle \mathbf{f}_i(\mathbf{k},\, t)\mathbf{f}_j(\mathbf{k}',\, t')\rangle \;\; = \;\; Ak^{4-d-y}\mathcal{P}_{ij}(\mathbf{k})\delta(\mathbf{k}+\mathbf{k}')\delta(t-t')$$

  where d is the dimensionality of the system and $\mathcal{P}_{ij}(\mathbf{k})$ is the transverse projection operator which enforces incompressibility.

- y is a control parameter.

Historical perspectives/Motivation

- One-loop RG studies of this 3D RFNSE[1] predict the energy spectrum to scale as $E(k) \sim k^{1-2y/3}$, which yields K41 scaling, i.e. $E(k) \sim k^{-5/3}$, when y = 4.
- Strictly speaking, the 3D RFNSE does not belong to same universality class as the 3D Navier-Stokes (3DNSE) equation because of logarithmic corrections to the energy flux in the inertial range.
- However, for y = 4, the 3D RFNSE and 3DNSE belong to the same universality class, to the extent that the exponent ratios are equal in both cases.

[1] V. Yakhot and S. A. Orszag, Phys. Rev. Lett. 57, 1722 (1986); J. K. Bhattacharjee, J. Phys. A 21, L551 (1988)

Historical perspectives/Motivation

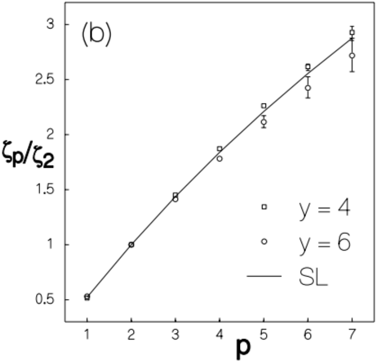

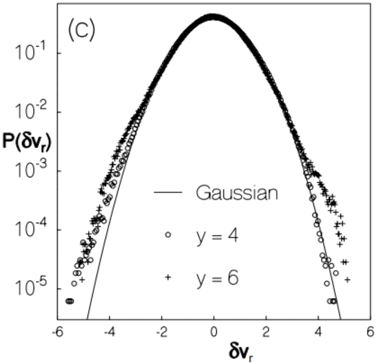

Multiscaling of velocity structure functions in 3D RFNSE, as illustrated in *A. Sain, Manu, and R. Pandit, Phys. Rev. Lett. 81, 4377 (1998)*.

Historical perspectives/Motivation

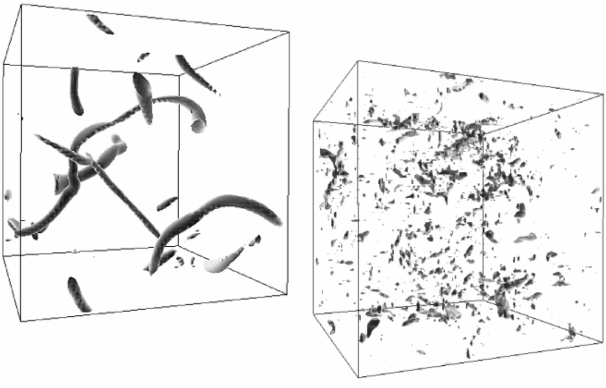

FIG. 3. Iso-$|\omega|$ surfaces obtained from instantaneous snapshots of the vorticity fields showing filaments for the 3DNSE (left) and no filaments for the RFNSE with $y = 4$ (right).

Disintegration of vorticity isosurfaces in 3D RFNSE, as illustrated in *A. Sain, Manu, and R. Pandit, Phys. Rev. Lett. 81, 4377 (1998)*.

Historical perspectives/Motivation

- This was confirmed via subsequent higher resolution numerical studies by Biferale, Cencini, Lanotte, Sbragaglia, and Toschi.

New Journal of Physics
An Institute of Physics and Deutsche Physikalische Gesellschaft Journal

Anomalous scaling and universality in hydrodynamic systems with power-law forcing

L Biferale[1], M Cencini[2,3,7], A S Lanotte[4,5], M Sbragaglia[1] and F Toschi[5,6]

[1] Dipartimento di Fisica and INFM, Università 'Tor Vergata', Via della Ricerca Scientifica 1, I-00133 Roma, Italy
[2] Center for Statistical Mechanics and Complexity, INFM Roma 1, Italy
[3] Dipartimento di Fisica, Università di Roma 'La Sapienza', Piazzale Aldo Moro, 2, I-00185 Roma, Italy
[4] Istituto per le Scienze dell'Atmosfera e del Clima, CNR, Str. Prov. Lecce-Monteroni km. 1.200, I-73100 Lecce, Italy
[5] INFM UDR Tor Vergata
[6] Istituto per le Applicazioni del Calcolo, CNR, Viale del Policlinico 137, I-00161 Roma, Italy
E-mail: massimo.cencini@roma1.infn.it

New Journal of Physics **6** (2004) 37
Received 14 January 2004
Published 18 March 2004
Online at http://www.njp.org/ (DOI: 10.1088/1367-2630/6/1/037)

Historical perspectives/Motivation

- Similar studies have been carried out for other randomly forced models too:
  - The Kardar-Parisi-Zhang (KPZ) equation.
  - The stochastically forced Burgers equation.

Historical perspectives/Motivation

VOLUME 56, NUMBER 9 PHYSICAL REVIEW LETTERS 3 MARCH 1986

Dynamic Scaling of Growing Interfaces

Mehran Kardar
Physics Department, Harvard University, Cambridge, Massachusetts 02138

Giorgio Parisi
Physics Department, University of Rome, I-00173 Rome, Italy

and

Yi-Cheng Zhang
Physics Department, Brookhaven National Laboratory, Upton, New York 11973
(Received 12 November 1985)

PHYSICAL REVIEW E VOLUME 52, NUMBER 5 NOVEMBER 1995

Kolmogorov turbulence in a random-force-driven Burgers equation: Anomalous scaling and probability density functions

Alexei Chekhlov and Victor Yakhot
Program in Applied and Computational Mathematics, Princeton University, Princeton, New Jersey 08544
(Received 6 April 1995)

Historical perspectives/Motivation

PHYSICAL REVIEW E VOLUME 56, NUMBER 4 OCTOBER 1997

From scaling to multiscaling in the stochastic Burgers equation

F. Hayot and C. Jayaprakash
Department of Physics, The Ohio State University, Columbus, Ohio 43210
(Received 23 May 1997)

PRL **94,** 194501 (2005) PHYSICAL REVIEW LETTERS week ending 20 MAY 2005

Is Multiscaling an Artifact in the Stochastically Forced Burgers Equation?

Dhrubaditya Mitra,[1,2] Jérémie Bec,[2,3] Rahul Pandit,[1,*] and Uriel Frisch[2]
[1]*Centre for Condensed Matter Theory, Department of Physics, Indian Institute of Science, Bangalore 560012, India*
[2]*Département Cassiopée, Observatoire de la Côte d'Azur, BP4229, 06304 Nice Cedex 4, France*
[3]*Dipartimento di Fisica, Università La Sapienza, Piazzale Aldo Moro 2, 00185 Roma, Italy*
(Received 23 June 2004; revised manuscript received 22 February 2005; published 16 May 2005)

Historical perspectives/Motivation

- Mathematical aspects of the KPZ equation:

Invent. math. (2014) 198:269–504
DOI 10.1007/s00222-014-0505-4

A theory of regularity structures

M. Hairer

Received: 1 October 2013 / Accepted: 21 January 2014 / Published online: 14 March 2014

Outline

- Kuramoto-Sivashinsky (KS) and KPZ equations
  - Model equations
  - 1D KPZ universality class
  - Numerical results
- 1D stochastic Burgers equation
  - Model equation
  - Numerical results for different power-law forcing
- Randomly-forced 1D Burgers MHD
  - Model equations
  - Numerical results
- Randomly-forced 3D MHD
  - Model equations
  - Numerical results

1D Kuramoto-Sivashinsky (KS) equation

- Deterministic 1D, KS PDE[1]:

$$\boxed{\frac{\partial h}{\partial t} + \frac{\partial^2 h}{\partial x^2} + \frac{\partial^4 h}{\partial x^4} + \frac{1}{2}\left(\frac{\partial h}{\partial x}\right)^2 = 0}$$

where $h(x,t) :=$ interfacial height profile, $L :=$ the system size (only control parameter).

- Studied in (a) chemical waves, (b) flame-front propagation, and (c) thin fluid film flow.
- Forcing comes from linear instability: low-wave-number modes are unstable, and high-wave-number modes are dissipative.
- Rich dynamical behaviours: in particular, for large L, it displays *spatiotemporal chaos* (reminiscent of turbulence)[2].

[1] Y Kuramoto and T Tsuzuki (1976) Prog. Theor. Phys. 55, 356; GI Sivashinsky (1979) Acta Astronautica 6, 560

[2] JM Hyman, B Nicolaenko and S Zaleski (1986) Vol. 23, 265-292

1D Kardar-Parisi-Zhang (KPZ) equation

- One-dimensional (1D) KPZ stochastic, nonlinear PDE:

$$\boxed{\frac{\partial h}{\partial t} = \nu \frac{\partial^2 h}{\partial x^2} + \frac{1}{2}\lambda \left(\frac{\partial h}{\partial x}\right)^2 + \sqrt{D}\eta}$$

  $h(x,t)$: interfacial height profile; ν, λ, and D are parameters; and η is a zero-mean Gaussian white noise.

- Studied by Kardar, Parisi, and Zhang[1] in 1986 to model a growing interface.
- Related models[2]:
  - poly-nuclear growth (PNG) model
  - weakly asymmetric simple exclusion process (WASEP)
  - directed polymers in random media (DPRM)

[1] M Kardar, G Parisi, and Y Zhang (1986) Phys. Rev. Lett. 59 889

[2] I Corwin (2011) arXiv:1106.1596; T Halpin-Healy, and K A Takeuchi (2015) J. Stat. Phys. 160, 794-814

1D KPZ universality class

- KPZ scaling: the large-time t height profile $h(x,t)$ in Eq. (20):

$$h(x,t) - h(x,0) \approx v_\infty t + (\Gamma t)^{\beta_{\mathrm{KPZ}}}\chi + o(t^{\beta_{\mathrm{KPZ}}}) \ , \quad t \to \infty$$

v_∞ and Γ depend on ν, λ, and D.

- $\beta_{\mathrm{KPZ}} = 1/3$ and the dynamical exponent $z = 1/(2\beta_{\mathrm{KPZ}}) = 3/2$, which follows from the surface roughness or interfacial width $w_L(t)$:

$$w_L(t) = \sqrt{\langle (h(x,t) - \langle h(x,t)\rangle)^2\rangle} \sim t^{1/2z}$$

- χ has different limiting statistics, i.e., probability distribution functions (PDFs), for different initial conditions[1]:
  - IC1. Wedge $\rightarrow$ Tracy-Widom PDF for the Gaussian unitary ensemble (TW-GUE).
  - IC2. Flat $\rightarrow$ Tracy-Widom PDF for the Gaussian orthogonal ensemble (TW-GOE).

[1] M Prähofer and H Spohn (2000) Phys. Rev. Lett. 84, 4882-4885, T Halpin-Healy and Y Lin (2014) Phys. Rev. E 89, 010103(R)

Results

PHYSICAL REVIEW E **101**, 030103(R) (2020)

Rapid Communications

One-dimensional Kardar-Parisi-Zhang and Kuramoto-Sivashinsky universality class: Limit distributions

Dipankar Roy [*]
Department of Mathematics, Indian Institute of Science, Bangalore 560012, India

Rahul Pandit [†]
Centre for Condensed Matter Theory, Department of Physics, Indian Institute of Science, Bangalore 560012, India

(Received 29 August 2019; accepted 10 March 2020; published 27 March 2020)

Tracy-Widom and Baik-Rains distributions appear as universal limit distributions for height fluctuations in the one-dimensional Kardar-Parisi-Zhang (KPZ) *stochastic* partial differential equation (PDE). We obtain the same universal distributions in the spatiotemporally chaotic, nonequilibrium, but statistically steady state of the one-dimensional Kuramoto-Sivashinsky (KS) *deterministic* PDE, by carrying out extensive pseudospectral direct numerical simulations to obtain the spatiotemporal evolution of the KS height profile $h(x, t)$ for different initial conditions. We establish, therefore, that the statistical properties of the one-dimensional (1D) KS PDE in this state are in the 1D KPZ universality class.

DOI: 10.1103/PhysRevE.101.030103

Results: distributions for IC1 and IC2

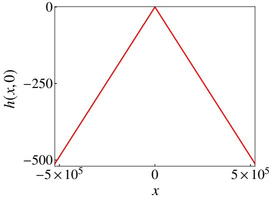

(a) IC1

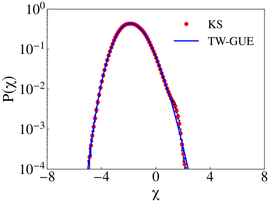

(b) PDF for IC1

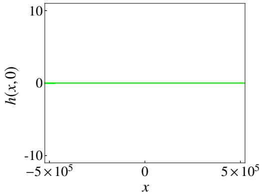

(c) IC2

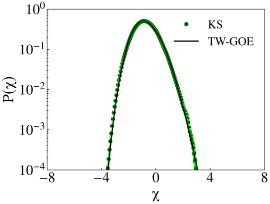

(d) PDF for IC2

Figures: Plots of $h(x,0)$ versus x for IC1 (a) and IC2 (c), and corresponding distributions of height fluctuations for IC1 (b) and IC2 (d).

The randomly forced Burgers model in 1D

- Recall the Burgers model[1] with random forcing in 1D:

$$\boxed{\frac{\partial u}{\partial t} + u\frac{\partial u}{\partial x} = \nu\frac{\partial^2 u}{\partial x^2} + f(x,t)}$$

where $u(x,t)$ is defined on $[0, 2\pi]$ with PBC; $f(x,t)$ is Gaussian and white-in-time with Fourier modes:

$$\langle \hat{f}(k,t)\hat{f}(k',t')\rangle = |k|^{\beta}\delta(k-k')\delta(t-t')$$

- One-loop perturbative RG expansion[2] yields the K41 energy spectrum $E(k) \sim k^{-5/3}$ for $\beta = -1$.
- In general, $E(k) \sim k^{-1+2\beta/3}$.

---

[1] J M Burgers (1948) Advances in Applied Mechanics, 1, 171-199
[2] A. Chekhlov and V. Yakhot, Phys. Rev. E 51, R2739 (1995)

The randomly forced Burgers model in 1D

- The velocity potential $\phi(x, t)$ is defined as $u(x, t) = -\partial_x \phi(x, t)$.
- For $\nu \to 0$ ($\nu \neq 0$), $\phi(x, t)$ can be determined from $\phi(x, t_0)$ by using the *Legendre transform*[1] (with no forcing between t_0 and t):

$$\phi(x, t) = \max_a \left(\phi(x, t_0) - \frac{(x-a)^2}{2(t-t_0)} \right).$$

[1] A Noullez, and M Vergassola (1994) J Sci Comput 9, 259–281

Results for $\beta = -1$ (reproduced[1])

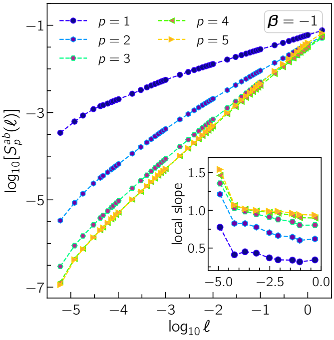

(a) Structure functions

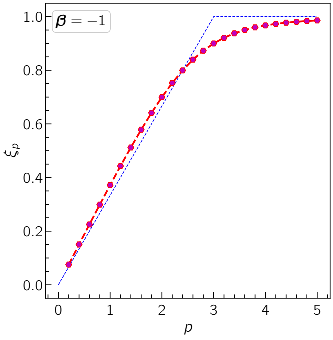

(b) Exponents

Figures: Plots of (a) structure functions (absolute value) versus ℓ and (b) exponents ξ_p versus p for $\beta = -1$, where the red points are the numerical data and the blue line is the bifractal behaviour

[1] D Mitra, J Bec, R Pandit, and U Frisch (2005) Phys. Rev. Lett. 94, 194501

Results for $\beta = -0.05$

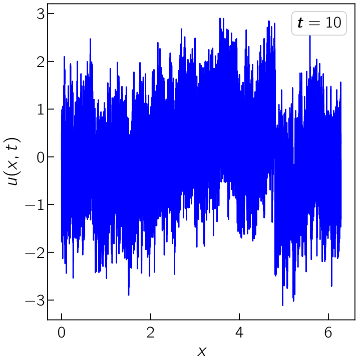

(a) Velocity profile

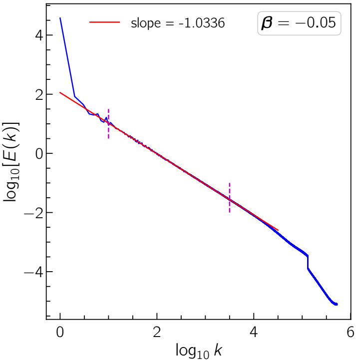

(b) Energy spectrum

Figures: Plots of (a) the non-equilibrium steady state velocity profile $u(x, t)$ and (b) the energy spectrum $E(k)$ for $\beta = -0.05$.

The energy spectrum in (b) follows the scaling law $E(k) \sim k^{-\sigma}$ where $\sigma = 1 - \frac{2\beta}{3}$.

Results for $\beta = -0.05$

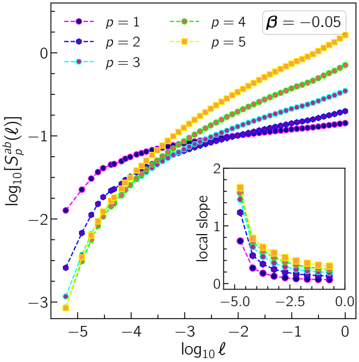

(a) Structure functions

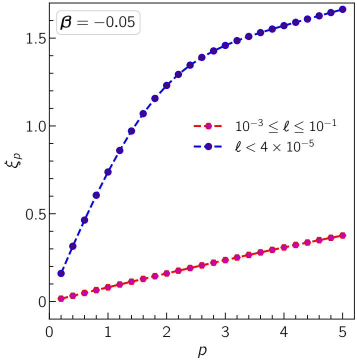

(b) Exponents

Figures: Plots of (a) structure functions (absolute value) versus ℓ and (b) exponents ξ_p versus p for $\beta = -0.05$.

The plot for ξ_p *suggests multifractal* behaviour for $\beta = -0.05$;
Note: Presence of simple and multiscaling regimes.

The Burgers MHD (BMHD) model

- De, Mitra and Pandit (in preparation).

The BMHD model[1] was originally introduced for studying compressible MHD turbulence in one spatial dimension.

$$\boxed{\begin{aligned} \frac{\partial u}{\partial t} + b_0 \frac{\partial b}{\partial x} + u \frac{\partial u}{\partial x} + b \frac{\partial b}{\partial x} &= \nu \frac{\partial^2 u}{\partial x^2} + f_u(x,t) \\ \frac{\partial b}{\partial t} + b_0 \frac{\partial u}{\partial x} + \frac{\partial}{\partial x}(ub) &= \mu \frac{\partial^2 b}{\partial x^2} + f_b(x,t) \end{aligned}}$$

$u(x,t)$ and $b(x,t)$ are the velocity and magnetic fields, respectively, at position x at time t, b_0 is the mean magnetic field, ν is the kinematic viscosity, μ is the magnetic diffusivity and, f_u and f_b are the external forces on the velocity and magnetic fields, respectively.

[1] J. H. Thomas, Phys. Fluids 11, 1245 (1968); J. Fleischer and P. H. Diamond, Phys. Rev. E 58, R2709 (1998); A. Basu, J. K. Bhattacharjee, and S. Ramaswamy, Eur. Phys. J. B 9, 725 (1999).

The Burgers MHD (BMHD) model

In terms of the Elsässer variables, $z^{\pm} = u \pm b$, the BMHD equations can be written as

$$
\begin{aligned}
\frac{\partial z^+}{\partial t} - b_0 \frac{\partial z^+}{\partial x} + z^+ \frac{\partial z^+}{\partial x} &= \nu_1 \frac{\partial^2 z^+}{\partial x^2} + \nu_2 \frac{\partial^2 z^-}{\partial x^2} + f^+(x,t) \\
\frac{\partial z^-}{\partial t} + b_0 \frac{\partial z^-}{\partial x} + z^- \frac{\partial z^-}{\partial x} &= \nu_1 \frac{\partial^2 z^-}{\partial x^2} + \nu_2 \frac{\partial^2 z^+}{\partial x^2} + f^-(x,t)
\end{aligned}
$$

where $\nu_1 = (\nu + \mu)/2$, $\nu_2 = (\nu - \mu)/2$ and $f^{\pm} = f_u \pm f_b$

The Burgers MHD (BMHD) model

- Magnetic Prandtl number $Pr_M = \nu/\mu$
- The BMHD equations are *Galilean invariant*.
- Conserves the 1D analogues of total energy and cross-helicity.
- When $Pr_M = 1$ i.e. $\nu = \mu$ and $b_0 = 0$, the BMHD equations de-couple into independent Burgers equations for $z^{\pm}$, which can be solved exactly for smooth initial conditions and forcing.
- Non-integrable when $Pr_M \neq 1$
- Can be used as a simple model for testing statistical theories of MHD turbulence

Random Power-law Forcing

- Gaussian, white-in-time, stochastic forcing $f_{u,\,b}(x,\,t)$ with Fourier space spectra, $\sim |k|^{\beta/2}$, and an infrared cut-off, $\lambda_c = N/8$, where N is the total number of available modes.
- The force correlations, in Fourier space, are as follows:

$$
\begin{aligned}
\langle f_u(k,t) f_u(k',t')\rangle &\sim |k|^{\beta}\delta(k+k')\delta(t-t') \\
\langle f_b(k,t) f_b(k',t')\rangle &\sim |k|^{\beta}\delta(k+k')\delta(t-t') \\
\langle f_u(k,t) f_b(k',t')\rangle &= 0
\end{aligned}
$$

- Forcing is in the form of periodic kicks or impulses.
- We choose $\beta = -1$ in our simulations.

RG Results

- One-loop perturbative RG study for $Pr_M = 1$ by Basu, Bhattacharjee and Ramaswamy, yields a K41 energy spectrum when $\beta = -1$

Eur. Phys. J. B 9, 725–730 (1999)

THE EUROPEAN PHYSICAL JOURNAL B
EDP Sciences

Mean magnetic field and noise cross-correlation in magnetohydrodynamic turbulence: results from a one-dimensional model

A. Basu[1,a], J.K. Bhattacharjee[2], and S. Ramaswamy[1,b]

[1] Department of Physics, Indian Institute of Science, Bangalore 560012, India
[2] Indian Association for the Cultivation of Science, Calcutta 700032, India

Received 29 October 1998 and Received in final form 8 December 1998

Numerical Procedure

- Pseudospectral method on a periodic domain of length $L = 2\pi$; $2/3$ dealiasing rule to remove aliasing errors.
- Implicit Euler method for time-marching between successive kicks.
- At the end of the n^{th} step, a term of the form $f(k, t_n)\sqrt{\delta t}$ is added to $u(x, t_n)$ and $b(x, t_n)$ in order to integrate the impulsive forcing.
- Range of Pr_M explored: $0.01 \leq Pr_M \leq 100$
- We have developed CUDA FORTRAN codes so as to be able to run our simulations on GPU clusters.

Quasi-Lagrangian (QL) framework

- Quasi-Lagrangian *(QL)* fields are calculated by tracking the motion of a mass-less tracer particle in the flow.
- If r is the displacement of the tracer, which initially was at some position R_0, then the quasi-Lagrangian field ϕ^{QL} is given by

$$\phi^{QL}(x,t) \;=\; \phi^{Eu}(x+r,t)$$

where $\phi^{Eu}(x,\ t)$ is the Eulerian field; ϕ can be u, b or $z^{\pm}$

- In Fourier space, $\phi^{QL}(k,\ t) = \left[\phi^{Eu}(k,\ t)\right] e^{ikr}$
- QL fields are necessary to extract dynamic multiscaling exponents. Eulerian fields exhibit trivial dynamic scaling behaviour due to *sweeping effects* which lead to random decorrelation of eddies.

Simulation parameters

Pr_M	ν	μ	δt	u_{rms}	b_{rms}	$L_{int,u}$	$L_{int,b}$	τ_u	τ_b
0.01	10^{-9}	10^{-7}	2×10^{-6}	0.20	0.11	0.85	0.64	$2.15\times10^{6}\delta t$	$2.95\times10^{6}\delta t$
0.1	10^{-8}	10^{-7}	2×10^{-6}	0.20	0.11	0.84	0.63	$2.15\times10^{6}\delta t$	$2.90\times10^{6}\delta t$
1	10^{-7}	10^{-7}	2×10^{-6}	0.20	0.11	0.85	0.63	$2.15\times10^{6}\delta t$	$2.90\times10^{6}\delta t$
10	10^{-7}	10^{-8}	2×10^{-6}	0.20	0.11	0.84	0.61	$2.15\times10^{6}\delta t$	$2.75\times10^{6}\delta t$
100	10^{-7}	10^{-9}	2×10^{-6}	0.20	0.11	0.85	0.59	$2.15\times10^{6}\delta t$	$2.65\times10^{6}\delta t$

δt is the time step size; u_{rms} and b_{rms} are the root-mean-square values of the velocity and magnetic fields of the flow, respectively; $L_{int,\,u}$ and $L_{int,\,b}$ are the integral length scales of the velocity and magnetic fields, respectively; $\tau_u = L_{int,\,u}/u_{rms}$ and $\tau_b = L_{int,\,b}/b_{rms}$ are the large-eddy turnover times associated with the velocity and magnetic fields, respectively. The simulations were performed at a high resolution of $N = 2^{20}$ grid points.

- Initial profiles:

$$u(x,0) = 0.2\sin(x-\pi/2)$$
$$b(x,0) = 0.1\sin(x-\pi/2)$$

Profiles

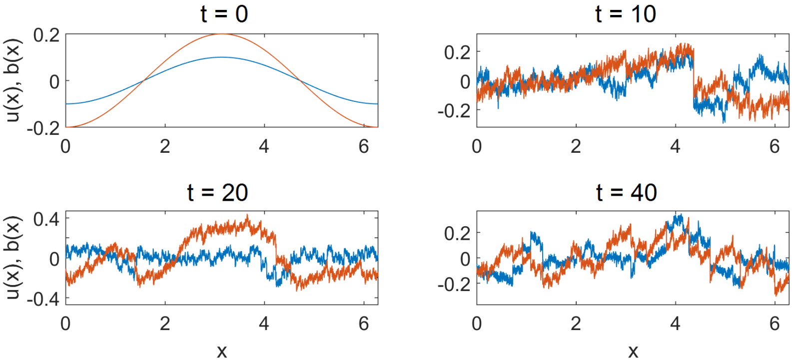

Velocity $(u(x, t))$ and *magnetic field $(b(x, t))$* profiles at the start of the simulation (t=0) and at subsequent times t.

Energy spectra

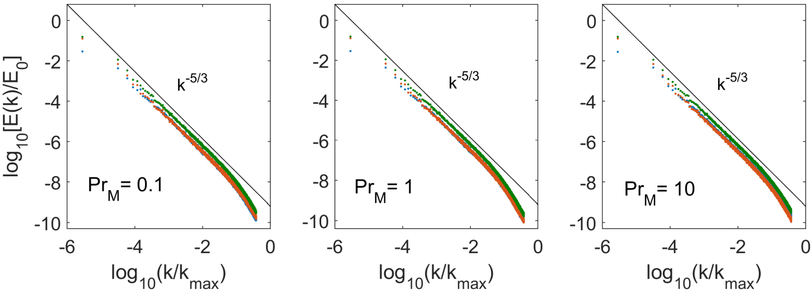

Normalized spectra $E(k)$ of *kinetic energy*, *magnetic energy* and *total energy*, for different Pr_M, plotted upto $k = \lambda_c$; $E_0 \equiv u_{rms}^2 + b_{rms}^2$ and $k_{max} = N/3$.

Equal-time Structure Functions

- We define equal-time structure functions of order p, of the field ϕ, as

$$S_p^{\phi}(r) = \langle |\delta\phi(r)|^p \rangle$$

  where $\delta\phi(r) = \phi(x + r) - \phi(x)$.
- For values of r within the inertial range, $\eta_{\phi} << r << L_{int,\phi}$,,

$$S_p^{\phi}(r) \sim r^{\zeta_p^{\phi}}$$

- Exponents ζ_p^{ϕ} are extracted from local slope analyses of log-log plots of $S_p^{\phi}(r)$ versus r, over more than a decade in r.

Equal-time Structure Functions

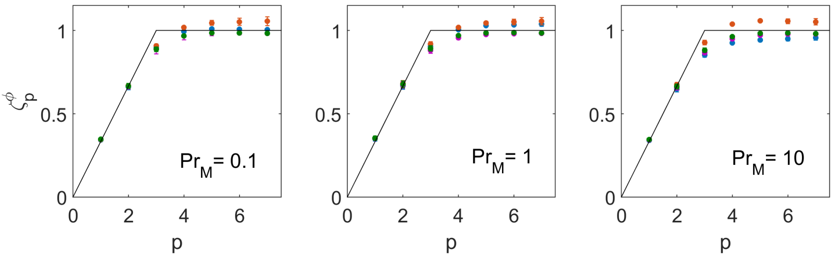

Exponents ζ_ϕ^p of u, b, z^+ and z^- for $p = 1$ to $p = 7$, at different Pr_M; the black lines represent bifractal behaviour; values of ζ_ϕ^p are the averages of the local slopes and the errorbars are the respective standard deviations.

Time-dependent Structure Functions

- We define normalized time-dependent structure functions of order p, of the field ϕ, as

$$F_p^{\phi}\left(r,\{t_1,t_2,...,t_p\}\right) = \frac{1}{S_p^{\phi}(r)}\langle|\delta\phi(r,t_1)...\delta\phi(r,t_p)|\rangle$$

- For simplicity, we choose $t_1 = t_2 = ... = t_{p-1} = 0$ and $t_p = t$
- At $t = 0$, $F_p^{\phi}(r,\, t) = 1$ for every r

Time-dependent Structure Functions

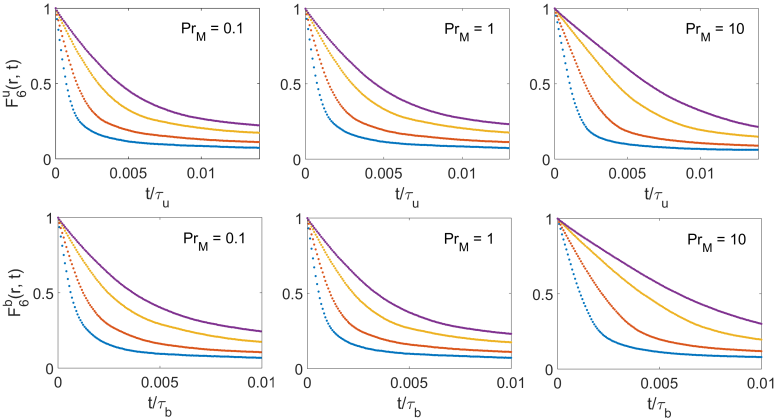

Variation of $F_b^6(r, t)$ and $F_u^6(r, t)$ with t for $rN/L = 100$, 200, 400 and 600, at different values of Pr_M.

Dynamic Multiscaling

- We define the integral time scale of order-p and degree-M, for the field ϕ, as

$$T^{I,\phi}_{p,M}(r) = \left[\int_0^{\tau^{\phi}} F^{\phi}_p(r,t)\, t^{M-1} dt\right]^{1/M}$$

- As per the dynamic scaling Ansatz, for values of r within the inertial range,

$$T^{I,\phi}_{p,M}(r) \sim r^{\chi^{I,\phi}_{p,M}}$$

- The dynamic multiscaling exponents $\chi^{I,z^{\pm}}_{p,M}$ can be shown to satisfy the linear bridge relations

$$\chi^{I,z^{\pm}}_{p,M} = 1 + \left(\zeta^{z^{\pm}}_{p-M} - \zeta^{z^{\pm}}_{p}\right)/M$$

Dynamic Multiscaling

- We calculate $\chi_{p,1}^{I,\phi}$ from local slope analyses of log-log plots of $T_{p,1}^{I,\phi}(r)$ versus r, over more than a decade in r.
- We choose τ^{ϕ} such that $F_p^{\phi}(r, \tau^{\phi}) = \epsilon$, for every r and p.
- Our results remain unchanged within errorbars for $0.9 < \epsilon < 0.95$.

Dynamic Multiscaling

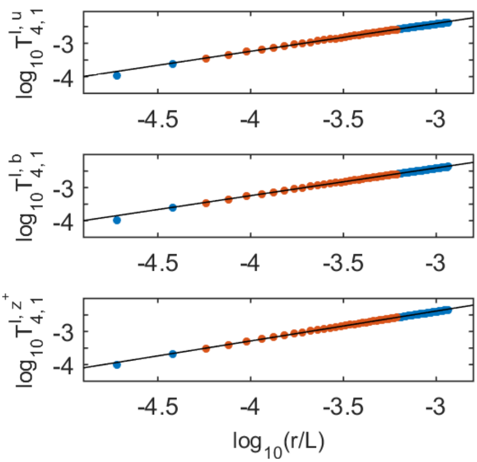

Log-log plots of $T^{l,\phi}_{p,1}$ versus r/L for $p = 4$ at $Pr_M = 1$; red points denote the region of local slope analysis; the black lines are the best-fits to the red regions.

Dynamic Multiscaling

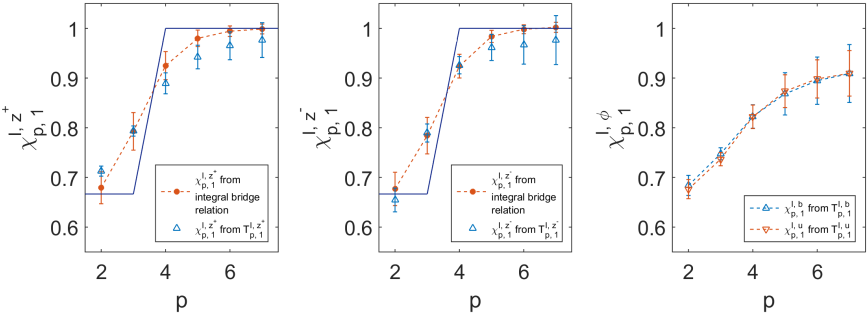

Dynamic multiscaling exponents, $\chi^{I,\phi}_{p,1}$, for $p = 2$ to $p = 6$ at $Pr_M = 1$.

- First two figures from the left: A comparison of $\chi^{I,z^{\pm}}_{p,1}$ with those predicted from the integral bridge relations involving (a) the equal-time exponents ζ^{ϕ}_{p} (red dashed lines) and (b) the bifractal exponents (blue solid lines).

Dynamic Multiscaling

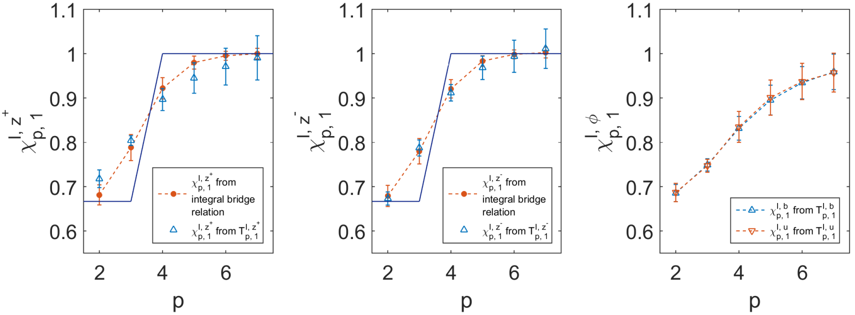

Dynamic multiscaling exponents, $\chi^{I,\phi}_{p,1}$, for $p = 2$ to $p = 6$ at $Pr_M = 0.1$.

- First two figures from the left: A comparison of $\chi^{I,z^\pm}_{p,1}$ with those predicted from the integral bridge relations involving (a) the equal-time exponents ζ^ϕ_p (red dashed lines) and (b) the bifractal exponents (blue solid lines).

Dynamic Multiscaling

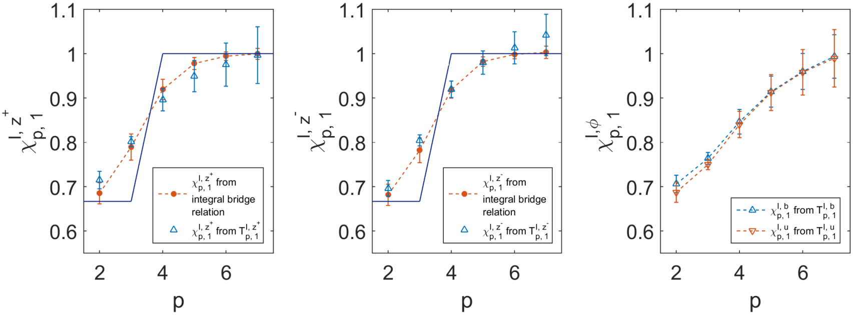

Dynamic multiscaling exponents, $\chi^{I,\phi}_{p,1}$, for $p = 2$ to $p = 6$ at $Pr_M = 10$.

- First two figures from the left: A comparison of $\chi^{I,z^\pm}_{p,1}$ with those predicted from the integral bridge relations involving (a) the equal-time exponents ζ^{ϕ}_{p} (red dashed lines) and (b) the bifractal exponents (blue solid lines).

Results

- Infinite number of time scales and dynamic exponents needed to characterize BMHD turbulence - evidence of *dynamic multiscaling*.
- Integral time exponents of $z^{\pm}$ seem to satisfy the integral bridge relations - note that $z^{\pm}$ have the same nonlinearity and inertial-range behaviour as the velocity in the Burgers equation.
- Cannot find such bridge relations for u and b because of the cross-coupling between these fields.

3D Randomly-forced MHD Turbulence

Direct Numerical Simulations of Three-dimensional Magnetohydrodynamic Turbulence with Random, Power-law Forcing

Ganapati Sahoo [1], Nadia Bihari Padhan [2], Abhik Basu [3], and Rahul Pandit [2,4]

[1] Department of Mathematics and Statistics, University of Helsinki

[2] Centre for Condensed Matter Theory, Department of Physics, Indian Institute of Science, Bangalore 560012, India.

[3] Theoretical Condensed Matter Physics Division, Saha Institute of Nuclear Physics, Calcutta, India.

[4] Also at: Jawaharlal Nehru Centre for Advanced Scientific Research, Jakkur, Bangalore, India

E-mail: `ganapati.sahoo@gmail.com`; `nadia@iisc.ac.in`; `abhik123@gmail.com`; `rahul@iisc.ac.in`

Abstract. We present pseudospectral direct-numerical-simulation (DNS) studies of the three-dimensional magnetohydrodynamic (MHD) equations (3DRFMHD) with a stochastic force that has zero mean and a variance $\sim k^{-3}$, where k is the wavenumber, because 3DRFMHD is used in field-theoretic studies of the scaling of energy spectra in MHD turbulence. We obtain velocity and magnetic-field spectra and structure functions and, from these, the multiscaling exponent ratios ζ_p/ζ_3, by using the extended self similarity (ESS) procedure. These exponent ratios lie within error bars of their counterparts for conventional three-dimensional MHD turbulence (3DMHD). We then carry out a systematic comparison of the statistical properties of 3DMHD and 3DRFMHD turbulence by examining various probability distribution functions (PDFs), joint PDFs, and isosurfaces of of, e.g., the moduli of the vorticity and the current density for three magnetic Prandtl numbers $\mathrm{Pr_M} = 0.1,\ 1,$ and 10.

PACS numbers:

3D Randomly-forced MHD Turbulence

Model equations:

$$\boxed{\begin{aligned}\frac{\partial \mathbf{u}}{\partial t} + (\mathbf{u}\cdot\nabla)\mathbf{u} &= \nu\nabla^2\mathbf{u} - \nabla\bar{P} + (\mathbf{b}\cdot\nabla)\mathbf{b} + \mathbf{f}_u \\ \frac{\partial \mathbf{b}}{\partial t} + (\mathbf{u}\cdot\nabla)\mathbf{b} &= (\mathbf{b}\cdot\nabla)\mathbf{u} + \eta\nabla^2\mathbf{b} + \mathbf{f}_b\end{aligned}}$$

$\mathbf{u}$ and $\mathbf{b}$ are velocity and magnetic field. $\omega = \nabla \times \mathbf{u}$ and $\mathbf{j} = \nabla \times \mathbf{b}$ are vorticity field and current density. Effective pressure is $\bar{P} = P + (b^2/8\pi)$, where P is the pressure.

Incompressibility:

$$\nabla \cdot \mathbf{u} = \mathbf{0}; \qquad \nabla \cdot \mathbf{b} = \mathbf{0}$$

Random, power-law forcing:

- The external forces f_u and f_b are zero-mean, Gaussian random forces that are uncorrelated with each other and delta correlated in time.

$$
\begin{aligned}
\langle \hat{f}_{u,m}(\mathbf{k},t)\hat{f}_{u,n}(\mathbf{k}',t')\rangle &= 2D_u k^{-3}\mathcal{P}_{m,n}(\mathbf{k})\delta(\mathbf{k}+\mathbf{k}')\delta(t-t') \\
\langle \hat{f}_{b,m}(\mathbf{k},t)\hat{f}_{b,n}(\mathbf{k}',t')\rangle &= 2D_b k^{-3}\mathcal{P}_{m,n}(\mathbf{k})\delta(\mathbf{k}+\mathbf{k}')\delta(t-t')
\end{aligned}
$$

- The transverse projector $\mathcal{P}_{m,n} \equiv [\delta_{m,n} - (k_m k_n/k^2)]$ ensures that $\nabla \cdot \mathbf{u} = \mathbf{0}$ and $\nabla \cdot \mathbf{b} = \mathbf{0}$.
- D_u and D_b are measures of the kinetic and magnetic energy injections. In our simulations, $D_u = D_b$.
- We do not consider cross correlations between $\mathbf{f}_u$ and $\mathbf{f}_b$ here.

RG results

- One-loop perturbative RG analysis of this model yields a K41 energy spectrum for $Pr_M = 1$ when the force autocorrelations scale as k^{-3}.

ELSEVIER

Available online at www.sciencedirect.com

SCIENCE DIRECT

Physics Reports 401 (2004) 229–380

PHYSICS REPORTS

www.elsevier.com/locate/physrep

Statistical theory of magnetohydrodynamic turbulence: recent results

Mahendra K. Verma

Department of Physics, Indian Institute of Technology, Kanpur 208016, India

Accepted 4 July 2004
editor: I. Procaccia

RG results

- Some more related research:
  - J.-D Fournier , P.-L Sulem, and A. Pouquet, J. Phys. A: Math. Gen. 15, 1393 (1982).
  - L. Ts. Adzhemyan, A. N. Vasil'ev, and M. Hnatich, Teoreticheskayai Matematicheskaya Fizika 64, 196 (1985); L. Ts. Adzhemyan, J. Honkonen, M. V. Kompaniets, A. N. Vasil'ev, Phys. Rev. E 71, 036305 (2005).
  - M. Hnatic, D. Horvath, R. Semancik, and M. Stehlik, Czech. J. Phys. 45, 91 (1995).
  - M. Hnatic, J. Honkonen, and M. Jurcisin, Phys. Rev. E 64, 056411 (2001).
  - C. B. Kim, Physics of Plasmas 11, 934 (2004).
  - C. B. Kim, and T. J. Yang, Physics of Plasmas 6, 2714 (1999).
  - Y. Zhou and G. Vahala, J. Plasma Phys. 39, 511 (1988).
  - Y. Zhou, Phys. Rep. 488, 1-49 (2010).

Direct Numerical Simulations (DNSs)

- Pseudospectral method with 2/3 dealiasing.
- Initial conditions:

$$E_u^0(k) = E_b^0(k) = E^0 k^4 \exp(-2k^2)$$

- Periodic boundary conditions with cubic box of side 2π and 512^3 collocation points.
- Simulation parameters:
  1. $\nu = 10^{-4}$, $\eta = 10^{-3}$, $\mathrm{Pr_M} = 0.1$, $\mathrm{Re}_\lambda \simeq 200$;
  2. $\nu = 10^{-3}$, $\eta = 10^{-3}$, $\mathrm{Pr_M} = 1$, $\mathrm{Re}_\lambda \simeq 50$;
  3. $\nu = 10^{-3}$, $\eta = 10^{-4}$, $\mathrm{Pr_M} = 10$, $\mathrm{Re}_\lambda \simeq 40$;
- $\mathrm{Pr_M} \equiv \mathrm{Re_M}/\mathrm{Re} = \nu/\eta$, the magnetic Prandtl number.
- Taylor-microscale Reynolds number $\mathrm{Re}_\lambda = u_{\mathrm{rms}}\lambda/\nu$.

Energy-time series

- Time evolution of kinetic energy, E_u, magnetic energy, E_b, and total energy, E.

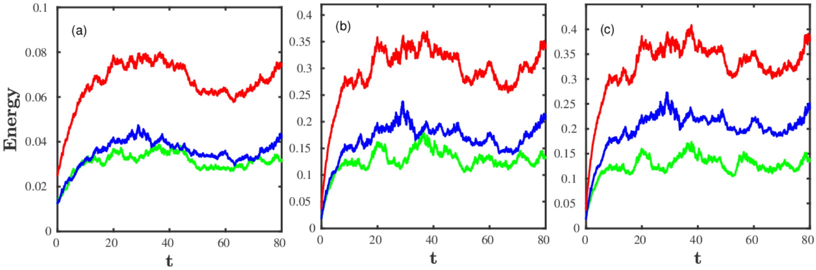

Figures: (a)$\mathrm{Pr_M} = 0.1$, (b) $\mathrm{Pr_M} = 1$ and (c) $\mathrm{Pr_M} = 10$.
(red line) $\rightarrow$ Total energy, E; (green line) $\rightarrow$ Kinetic energy, E_u;
(blue line) $\rightarrow$Magnetic energy, E_b.

- A statistically steady state is obtained, even for 3DRFMHD, in which E, E_u, and E_b fluctuate about their mean

K.E spectra

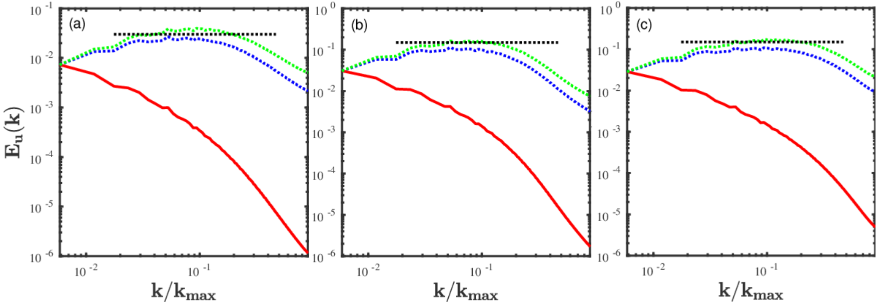

Figures: (a)$\mathrm{Pr_M} = 0.1$, (b) $\mathrm{Pr_M} = 1$ and (c) $\mathrm{Pr_M} = 10$.
(red line) $\longrightarrow$ kinetic energy spectra $E_u(k)$; (green line) $\longrightarrow$ compensated spectra $k^{5/3}E_u(k)$; (blue line) $\longrightarrow$ compensated spectra $k^{3/2}E_u(k)$.

Magnetic energy spectra

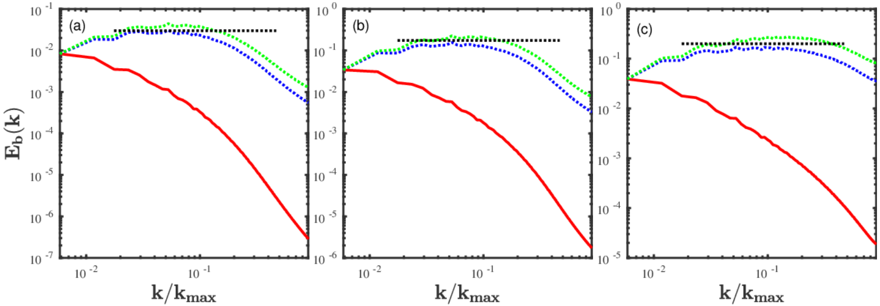

Figures: (a)$\mathrm{Pr_M} = 0.1$, (b) $\mathrm{Pr_M} = 1$ and (c) $\mathrm{Pr_M} = 10$.
(red line) $\longrightarrow$ Magnetic energy spectra $E_b(k)$; (green line) $\longrightarrow$ compensated spectra $k^{5/3}E_b(k)$; (blue line) $\longrightarrow$ compensated spectra $k^{3/2}E_b(k)$.

Dissipation-time series

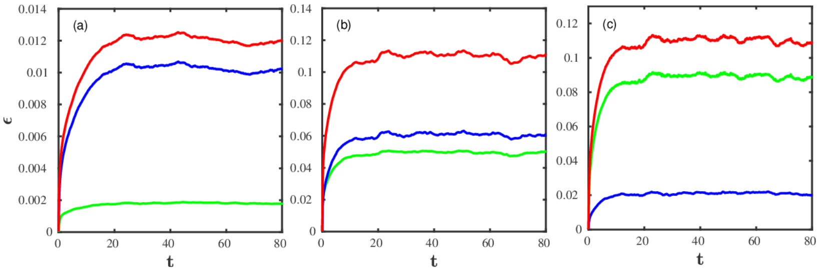

Figures: (a)$\mathrm{Pr_M} = 0.1$, (b) $\mathrm{Pr_M} = 1$ and (c) $\mathrm{Pr_M} = 10$.
(red line) $\rightarrow$ Total energy dissipation rate, ϵ; (green line) $\rightarrow$ Kinetic energy dissipation rate, ϵ_u; (blue line) $\rightarrow$Magnetic energy dissipation rate, ϵ_b.

Dissipation spectra

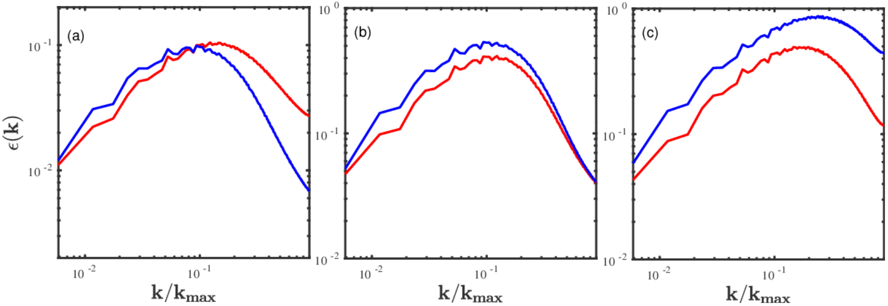

Figures: (a)$\mathrm{Pr_M} = 0.1$, (b) $\mathrm{Pr_M} = 1$ and (c) $\mathrm{Pr_M} = 10$.
(red line) $\rightarrow$ Kinetic energy dissipation spectra, $\epsilon_u(k)$;
(blue line) $\rightarrow$Magnetic energy dissipation spectra, $\epsilon_b(k)$.

Pressure spectra

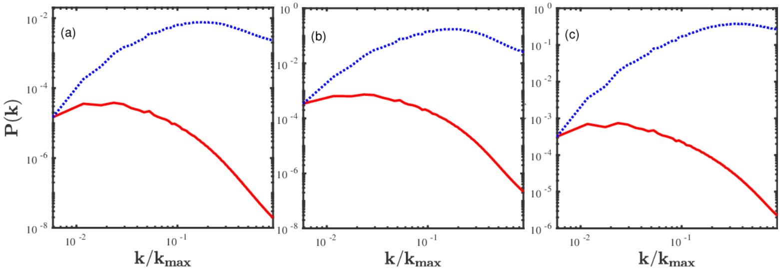

Figures: (a)$\mathrm{Pr_M} = 0.1$, (b) $\mathrm{Pr_M} = 1$ and (c) $\mathrm{Pr_M} = 10$.
(red line) $\rightarrow$ Effective pressure spectra, $P(k)$;
(blue line) $\rightarrow$compensated spectra $k^{7/3}P(k)$.

Isosurface plots of vorticity and current density

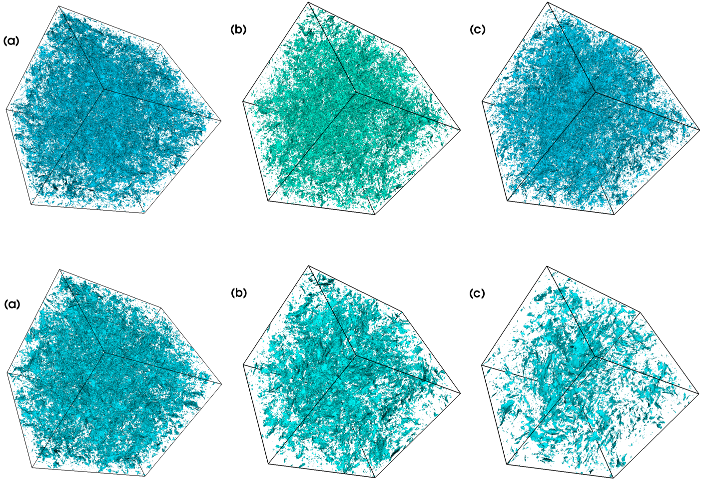

Figures: (a)$\mathrm{Pr_M} = 0.1$, (b) $\mathrm{Pr_M} = 1$ and (c) $\mathrm{Pr_M} = 10$.
Isosurfaces of the modulus of the vorticity ω (1st row) and current j (2nd row)in 3DRFMHD. The values of ω and j, we consider here, are two standard deviations more than its mean value.

PDFs of velocity- and magnetic-field increments

- $\delta \mathbf{a}_{\|}(\mathbf{x}, \mathbf{l}) \equiv \mathbf{a}(\mathbf{x}+\mathbf{l}, \mathbf{t}) - \mathbf{a}(\mathbf{x}, \mathbf{t})] \cdot \frac{\mathbf{l}}{|\mathbf{l}|}$, $\mathbf{a}$ is either $\mathbf{u}$ or $\mathbf{b}$

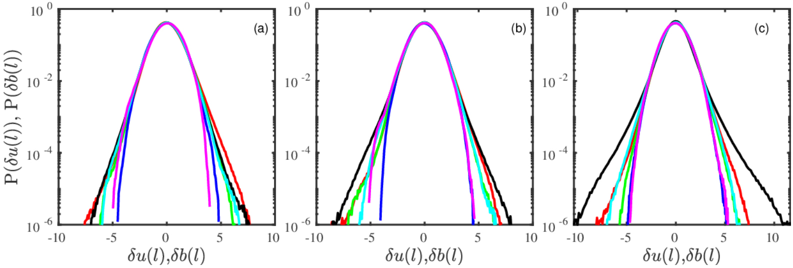

Figures: (a)$\mathrm{Pr_M} = 0.1$, (b) $\mathrm{Pr_M} = 1$ and (c) $\mathrm{Pr_M} = 10$. Semilog (base 10) plots of PDFs of velocity increments $\delta u(l)$, for separations $l = 2\delta x$ (red lines), $10\delta x$ (green lines), and $100\delta x$ (blue lines), and of magnetic-field increments $\delta b(l)$, for separations $l = 2\delta x$ (black lines), $10\delta x$ (cyan lines), and $100\delta x$ (magenta lines).

- Arguments of these PDFs are scaled by their root-mean-square values.

Structure functions

- The scale dependence of order-p equal-time, longitudinal velocity and magnetic field structure functions:

  $$S^u_p(l) \equiv \langle|\delta u_{\|}(\mathbf{x},\mathbf{l})|^{\mathbf{p}}\rangle,\ S^b_p(l) \equiv \langle|\delta b_{\|}(\mathbf{x},\mathbf{l})|^{\mathbf{p}}\rangle$$
  $$\delta u_{\|}(\mathbf{x},\mathbf{l}) \equiv \mathbf{u}(\mathbf{x}+\mathbf{l},\mathbf{t}) - \mathbf{u}(\mathbf{x},\mathbf{t})] \cdot \frac{\mathbf{l}}{|\mathbf{l}|},$$
  $$\delta b_{\|}(\mathbf{x},\mathbf{l}) \equiv \mathbf{b}(\mathbf{x}+\mathbf{l},\mathbf{t}) - \mathbf{b}(\mathbf{x},\mathbf{t})] \cdot \frac{\mathbf{l}}{|\mathbf{l}|}$$

- For the inertial range $\eta^u_d, \eta^b_d \ll l \ll L$, we expect $S^u_p(l) \sim l^{\zeta^u_p}$ and $S^b_p(l) \sim l^{\zeta^b_p}$, where ζ^u_p and ζ^b_p are inertial-range multiscaling exponents for velocity and magnetic fields.

Structure functions

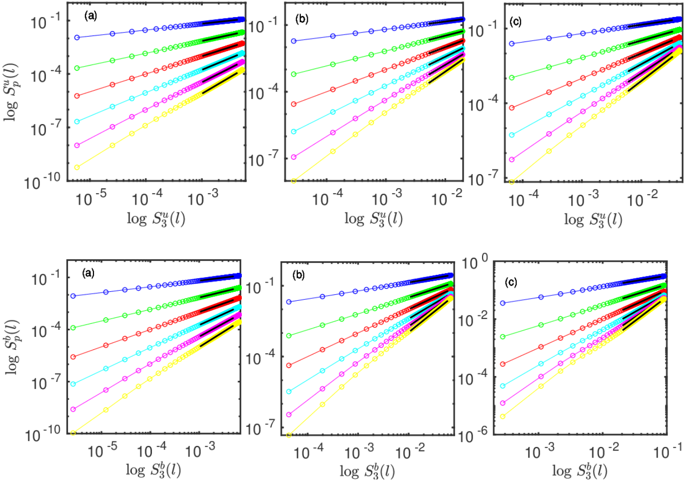

Figures: (a)$\mathrm{Pr_M} = 0.1$, (b) $\mathrm{Pr_M} = 1$ and (c) $\mathrm{Pr_M} = 10$.
Log-log (base 10) extended-self-similarity (ESS) plots of velocity and magnetic field structure functions of order p versus that of order 3; $p = 1$ (blue), $p = 2$ (green), $p = 3$ (red), $p = 4$ (cyan), $p = 5$ (magenta), and $p = 6$ (yellow).

Multiscaling exponents

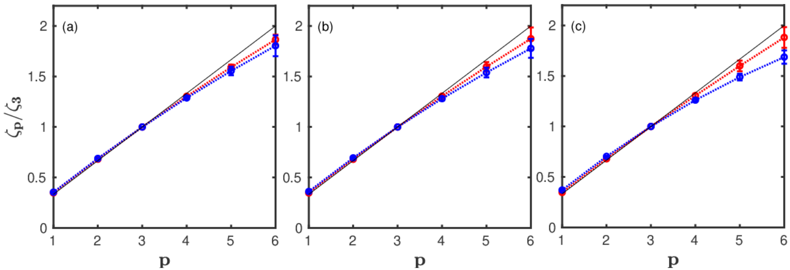

Figures: (a)$\mathrm{Pr_M} = 0.1$, (b) $\mathrm{Pr_M} = 1$ and (c) $\mathrm{Pr_M} = 10$.
Multiscaling exponent ratios ζ_p^u/ζ_3^u (red line) and ζ_p^b/ζ_3^b (blue line) versus p.

p	$\zeta_p^u/\zeta_3^u;\ \zeta_p^b/\zeta_3^b(\mathrm{Pr_M}=0.1)$	$\zeta_p^u/\zeta_3^u;\ \zeta_p^b/\zeta_3^b(\mathrm{Pr_M}=1)$	$\zeta_p^u/\zeta_3^u;\ \zeta_p^b/\zeta_3^b(\mathrm{Pr_M}=10)$
1	$0.35 \pm 0.00;\ 0.35 \pm 0.00$	$0.35 \pm 0.00;\ 0.36 \pm 0.00$	$0.35 \pm 0.01;\ 0.37 \pm 0.00$
2	$0.68 \pm 0.00;\ 0.69 \pm 0.00$	$0.68 \pm 0.00;\ 0.69 \pm 0.00$	$0.68 \pm 0.01;\ 0.70 \pm 0.00$
3	$1.00 \pm 0.00;\ 1.00 \pm 0.00$	$1.00 \pm 0.00;\ 1.00 \pm 0.00$	$1.00 \pm 0.00;\ 1.00 \pm 0.00$
4	$1.30 \pm 0.01;\ 1.29 \pm 0.01$	$1.30 \pm 0.01;\ 1.28 \pm 0.01$	$1.30 \pm 0.02;\ 1.26 \pm 0.01$
5	$1.59 \pm 0.03;\ 1.56 \pm 0.04$	$1.60 \pm 0.05;\ 1.53 \pm 0.05$	$1.60 \pm 0.05;\ 1.49 \pm 0.03$
6	$1.86 \pm 0.05;\ 1.80 \pm 0.10$	$1.87 \pm 0.11;\ 1.78 \pm 0.10$	$1.88 \pm 0.10;\ 1.69 \pm 0.07$

Hyperflatness

- We obtain the hyperflatnesses $F_6^u(l) = S_6^u(l)/[S_2^u(l)]^3$ and $F_6^b(l) = S_6^b(l)/[S_2^b(l)]^3$.

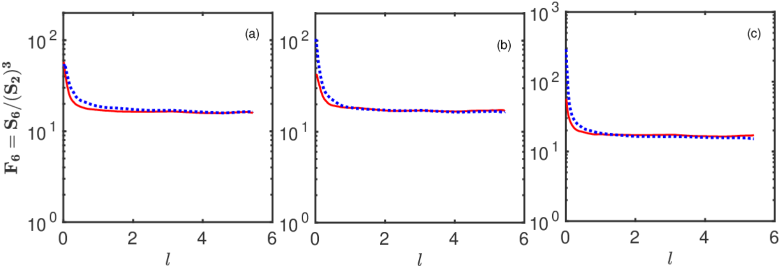

Figures: (a)$\mathrm{Pr_M} = 0.1$, (b) $\mathrm{Pr_M} = 1$ and (c) $\mathrm{Pr_M} = 10$.
Semilog (base 10) plots of the hyperflatness of the velocity field (red line) and its magnetic counterpart (blue dashed line)

Results

- Equal-time exponent ratios ζ_p/ζ_3 indicate that b is slightly more intermittent than u, which is also visible from PDFs of velocity and magnetic field increments.
- The random, power-law forcing leads to the destruction of the tube-like structures in isosurfaces of vorticity ω and current density $\mathbf{j}$.

Conclusions

- Direct numerical simulations indicate that turbulence with (spatial) power-law forcing has at least two different regimes (dependent on the power-law forcing): (a) with scale invariant statistics and (b) with multifractal statistics, i.e., broken scale invariance.
- Can these be studied by using a variant of theories of spontaneous stochasticity, rough paths, and regularity structures, as recently applied to the Kardar Parisi Zhang (KPZ) equation?
- There is a long tradition, in fluid mechanics, of including a driving force in the equations; here we investigate random driving forces.

THANK YOU FOR YOUR ATTENTION